Supplemental Materials
for

Ab initio Real-Time Quantum Dynamics of Charge Carriers in Momentum Space

Zhenfa Zheng[1], Yongliang Shi[1,2,3*], Jin-Jian Zhou[4], Oleg V. Prezhdo[5], Qijing Zheng[1*] and Jin Zhao[1,6*]

[1*] Department of Physics, ICQD/Hefei National Laboratory for Physical Sciences at Microscale, and CAS Key Laboratory of Strongly-Coupled Quantum Matter Physics, University of Science and Technology of China, Hefei, 230026, Anhui, China .

[2*] Center for Spintonics and Quantum Systerms, State Key Laboratory for Mechanical Behavior of Materials, School of Materials Science and Engineering, Xi'an Jiaotong University, Xi'an, 710049, Shanxi, China .

[3*] State Key Laboratory of Surface Physics and Department of Physics, Fudan University, Shanghai, 200433, China .

[4] School of Physics, Beijing Institute of Technology, Beijing, 100081, China .

[5] Departments of Chemistry, Physics, and Astronomy, University of Southern California, Los Angeles, 90089, California, USA .

[6*] Department of Physics and Astronomy, University of Pittsburgh, Pittsburgh, 15260, Pennsylvania, USA .

*Corresponding author(s). E-mail(s): sylcliff@xjtu.edu.cn; zqj@ustc.edu.cn; zhaojin@ustc.edu.cn;

1 Zero nonadiabatic coupling for Bloch states with different momenta

In the real-space *ab initio* nonadiabatic molecular dynamics (NAMD) approach (NAMD_**r**), the charge carrier dynamics is mainly determined by the nonadiabatic coupling (NAC), which can be written as:

$$\begin{aligned} d_{m\mathbf{k}',n\mathbf{k}} &= \langle\psi_{m\mathbf{k}'}|\frac{\mathrm{d}}{\mathrm{d}t}|\psi_{n\mathbf{k}}\rangle \\ &\approx \frac{\langle\psi_{m\mathbf{k}'}(t)|\psi_{n\mathbf{k}}(t+\Delta t)\rangle - \langle\psi_{m\mathbf{k}'}(t+\Delta t)|\psi_{n\mathbf{k}}(t)\rangle}{2\Delta t}. \end{aligned} \tag{S1}$$

For periodic systems, Bloch's theorem states that electronic state takes the form of a Bloch wave, i.e.

$$\psi_{n\mathbf{k}}(\mathbf{r}) = N_p^{-1/2} e^{i\mathbf{k}\cdot\mathbf{r}} u_{n\mathbf{k}}(\mathbf{r}), \tag{S2}$$

where $\mathbf{r}$ is the position of the electron, N_p is the number of unit cells, and $u_{n\mathbf{k}}(\mathbf{r})$ is a cell-periodic function, which satisfies

$$u_{n\mathbf{k}}(\mathbf{r}+\mathbf{L}_p) = u_{n\mathbf{k}}(\mathbf{r}), \tag{S3}$$

where $\mathbf{L}_p$ is the lattice vector of the p-th unit cell. Note that the Bloch wave $\psi_{n\mathbf{k}}$ is normalized in the Born-von Kármán (BvK) supercell, while the periodic part $u_{n\mathbf{k}}(\mathbf{r})$ is normalized in the unit cell. The overlap or inner product of two Bloch waves at different times becomes

$$\begin{aligned} \langle\psi_{m\mathbf{k}'}(t')|\psi_{n\mathbf{k}}(t)\rangle &= N_p^{-1} \int e^{-i(\mathbf{k}'-\mathbf{k})\cdot\mathbf{r}} u^*_{m\mathbf{k}'}(\mathbf{r})\, u_{n\mathbf{k}}(\mathbf{r})\, \mathrm{d}\mathbf{r} \\ &= N_p^{-1} \sum_p \int_{p\text{-cell}} e^{-i(\mathbf{k}'-\mathbf{k})\cdot(\mathbf{r}+\mathbf{L}_p)} u^*_{m\mathbf{k}'}(\mathbf{r}+\mathbf{L}_p)\, u_{n\mathbf{k}}(\mathbf{r}+\mathbf{L}_p)\, \mathrm{d}\mathbf{r} \\ &= N_p^{-1} \sum_p e^{-i(\mathbf{k}'-\mathbf{k})\cdot\mathbf{L}_p} \int_{\mathrm{uc}} e^{-i(\mathbf{k}'-\mathbf{k})\cdot\mathbf{r}} u^*_{m\mathbf{k}'}(\mathbf{r})\, u_{n\mathbf{k}}(\mathbf{r})\, \mathrm{d}\mathbf{r} \\ &= \delta_{\mathbf{k},\mathbf{k}'} \int_{\mathrm{uc}} e^{-i(\mathbf{k}'-\mathbf{k})\cdot\mathbf{r}} u^*_{m\mathbf{k}'}(\mathbf{r};\, t')\, u_{n\mathbf{k}}(\mathbf{r};\, t)\, \mathrm{d}\mathbf{r}, \end{aligned} \tag{S4}$$

where the subscripts "p-cell" and "uc" indicate that the integral is carried out within the p-th unit cell and the first unit cell, respectively. From the third line to the last line, we have used

$$N_p^{-1} \sum_p e^{-i(\mathbf{k}'-\mathbf{k})\cdot\mathbf{L}_p} = \delta_{\mathbf{k},\mathbf{k}'}. \tag{S5}$$

From Eq. (S4), one can see that the inner product of two Bloch states at different times is zero for $\mathbf{k}' \neq \mathbf{k}$, thus the relating NAC is also zero. Apparently,

this excludes the possibility of using a unit cell to perform NAMD calculations were one to include different Bloch states. To circumvent this problem, in the NAMD_**r** approach, by introducing a large enough supercell, one can effectively fold the electronic states of different momenta **k** to the Brillouin Zone center (Γ-point). Moreover, a large supercell can also accommodate phonon modes of different wavevectors **q**, which can compensate the momentum difference needed for the crystal momentum conservation, resulting in a non-zero overlap and hence a non-zero NAC between the states.

2 Solving the Time-dependent Kohn-Sham (TDKS) equation

For quantum dynamics of excited carrier, we solve the time-dependent Shrödinger equation (TDSE)

$$i\hbar\frac{\partial}{\partial t}\left|\Psi(\mathbf{r};\ \mathbf{R}(t))\right\rangle = \hat{H}^{el}(\mathbf{r};\ \mathbf{R}(t))\left|\Psi(\mathbf{r};\ \mathbf{R}(t))\right\rangle. \tag{S6}$$

Here, both electronic Hamiltonian $\hat{H}^{el}(\mathbf{r};\ \mathbf{R}(t))$ and electronic wavefunction $|\Psi(\mathbf{r};\ \mathbf{R}(t))\rangle$ depend on time through nuclear trajectory $\mathbf{R}(t)$.

In the nonadiabatic molecular dynamics simulation (NAMD) approach in momentum space (NAMD_**k**), starting with the equilibrium atomic structure $\mathbf{R}_0$, the electronic Hamiltonian can be separated into two parts

$$\hat{H}^{el}(\mathbf{r};\ \mathbf{R}(t)) = \hat{H}^{0}(\mathbf{r};\ \mathbf{R}_0) + \Delta\hat{H}(\mathbf{r};\ \mathbf{R}(t)), \tag{S7}$$

where the first part $\hat{H}^{0}(\mathbf{r};\ \mathbf{R}_0)$ is the Hamiltonian at equilibrium positions $\mathbf{R}_0$, which is time-independent. The second part $\Delta\hat{H}$ is the variation of Hamiltonian, which is induced by nuclear displacements $\Delta\mathbf{R}(t) = \mathbf{R}(t) - \mathbf{R}_0$. As the nuclear coordinates only appear in the potential term $V(\mathbf{r};\ \mathbf{R})$ in the electronic Hamiltonian $\hat{H}^{el} = \hat{T} + \hat{V}$, therefore $\Delta\hat{H}$ can be also written as

$$\Delta\hat{H}(\mathbf{r};\ \mathbf{R}(t)) = \Delta V(\mathbf{r};\ \mathbf{R}(t)) = V(\mathbf{r};\ \mathbf{R}(t)) - V(\mathbf{r};\ \mathbf{R}_0). \tag{S8}$$

Then, we expand the electronic wavefunction by the eigenstates of equilibrium structure Hamiltonian $\hat{H}^{0}(\mathbf{r};\ \mathbf{R}_0)$

$$\left|\Psi(\mathbf{r};\ \mathbf{R}(t))\right\rangle = \sum_{n\mathbf{k}} c_{n\mathbf{k}}(t)\left|\psi_{n\mathbf{k}}(\mathbf{r};\ \mathbf{R}_0)\right\rangle, \tag{S9}$$

where **k** represents the crystal momentum and n is the band index. The basis set $\left\{|\psi_{n\mathbf{k}}(\mathbf{r};\ \mathbf{R}_0)\rangle\right\}$ are calculated in the framework of Kohn-Sham (KS) density functional theory (DFT), and satisfy

$$\hat{H}^{0}(\mathbf{r};\ \mathbf{R}_0)\left|\psi_{n\mathbf{k}}\right\rangle = \epsilon_{n\mathbf{k}}\left|\psi_{n\mathbf{k}}\right\rangle, \tag{S10}$$

where $\epsilon_{n\mathbf{k}}$ is eigen-energy of KS state $|\psi_{n\mathbf{k}}\rangle$. Here, it should be emphasized that the basis wavefunctions $\{|\psi_{n\mathbf{k}}\rangle\}$ are *time-independent* while the expanding coefficients $c_{n\mathbf{k}}(t)$ are *time-dependent*.

By substituting Eq. (S7)-(S10) into Eq. (S6) and multiplying by $\langle\psi_{m\mathbf{k}'}|$ on both sides of equation, we get the time-dependent equation for the expanding coefficient

$$i\hbar\frac{\mathrm{d}}{\mathrm{d}t}c_{m\mathbf{k}'}(t) = \sum_{n\mathbf{k}}\left(H^0_{m\mathbf{k}',n\mathbf{k}} + H^{ep}_{m\mathbf{k}',n\mathbf{k}}\right)c_{n\mathbf{k}}(t), \tag{S11}$$

where $H^0_{m\mathbf{k}',n\mathbf{k}}$ is the matrix element of $\hat{H}^0$, which is apparently diagonal

$$H^0_{m\mathbf{k}',n\mathbf{k}} = \langle\psi_{m\mathbf{k}'}|\hat{H}^0|\psi_{n\mathbf{k}}\rangle = \epsilon_{n\mathbf{k}}\delta_{mn,\mathbf{k}'\mathbf{k}}, \tag{S12}$$

and $H^{ep}_{m\mathbf{k}',n\mathbf{k}}$ is the electron-phonon (*e-ph*) coupling matix element

$$H^{ep}_{m\mathbf{k}',n\mathbf{k}} = \langle\psi_{m\mathbf{k}'}|\Delta V|\psi_{n\mathbf{k}}\rangle\,. \tag{S13}$$

To calculate the *e-ph* term, we expand the potential energy $V(\mathbf{r};\ \mathbf{R}(t))$ in terms of nuclear displacements $\Delta\mathbf{R}(t)$. The potential to first order in displacements is

$$V(\mathbf{r};\ \mathbf{R}(t)) = V(\mathbf{r};\ \mathbf{R}_0) + \sum_{p\kappa}\left.\frac{\partial V(\mathbf{r};\ \mathbf{R})}{\partial\mathbf{R}_{p\kappa}}\right|_{\mathbf{R}=\mathbf{R}_0}\cdot\Delta\mathbf{R}_{p\kappa}(t). \tag{S14}$$

where the position of the nucleus κ in the p-th unit cell is denoted as $\mathbf{R}_{p\kappa} = \mathbf{L}_p + \tau_\kappa$, and $\mathbf{L}_p$ is the cell vector. In practice, it is convenient to decompose nuclear displacements $\Delta\mathbf{R}(t)$ into normal modes

$$\Delta\mathbf{R}_{p\kappa}(t) = \sqrt{\frac{M_0}{N_p M_\kappa}}\sum_{\mathbf{q}\nu}e^{i\mathbf{q}\cdot\mathbf{L}_p}\mathbf{e}_{\kappa\nu}(\mathbf{q})Q_{\mathbf{q}\nu}(t), \tag{S15}$$

where M_0 is an arbitrary reference mass introduced to ensure that both sides of the equation have the dimension of length. Typically, M_0 is chosen to be the proton mass. $\mathbf{e}_{\kappa\nu}(\mathbf{q})$ is the polarization of the vibration wave corresponding to the wave vector $\mathbf{q}$ and mode ν. $Q_{\mathbf{q}\nu}(t)$ is the normal mode coordinate of the corresponding mode. According to Eq. (S8),

$$\Delta V(\mathbf{r};\ \mathbf{R}(t)) = \sqrt{\frac{1}{N_p}}\sum_{\mathbf{q}\nu}\sum_{p\kappa}\sqrt{\frac{M_0}{M_\kappa}}e^{i\mathbf{q}\cdot\mathbf{L}_p}\left.\frac{\partial V(\mathbf{r};\ \mathbf{R})}{\partial\mathbf{R}_{p\kappa}}\right|_{\mathbf{R}=\mathbf{R}_0}\cdot\mathbf{e}_{\kappa\nu}(\mathbf{q})Q_{\mathbf{q}\nu}(t). \tag{S16}$$

Here, by defining

$$\partial_{\mathbf{q}\kappa}v(\mathbf{r};\ \mathbf{R}_0) = \sum_p e^{-i\mathbf{q}\cdot(\mathbf{r}-\mathbf{L}_p)}\left.\frac{\partial V(\mathbf{r};\ \mathbf{R})}{\partial\mathbf{R}_{p\kappa}}\right|_{\mathbf{R}=\mathbf{R}_0}, \tag{S17}$$

and

$$\Delta_{\mathbf{q}\nu} v(\mathbf{r};\ \mathbf{R}_0) = \sum_{\kappa} (M_0/M_\kappa)^{1/2} \partial_{\mathbf{q}\kappa} V(\mathbf{r};\ \mathbf{R}_0) \cdot \mathbf{e}_{\kappa\nu}(\mathbf{q}) l_{\mathbf{q}\nu}, \tag{S18}$$

where $l_{\mathbf{q}\nu}$ is the "zero-point" displacement amplitude:

$$l_{\mathbf{q}\nu} = \sqrt{\frac{\hbar}{2M_0\omega_{\mathbf{q}\nu}}} \tag{S19}$$

One can show that $\partial_{\mathbf{q}\kappa} v(\mathbf{r};\ \mathbf{R}_0)$ and $\Delta_{\mathbf{q}\nu} v(\mathbf{r};\ \mathbf{R}_0)$ are lattice-periodic functions. Then, Eq. (S16) can be written as

$$\Delta V(\mathbf{r};\ \mathbf{R}(t)) = N_p^{-1/2} \sum_{\mathbf{q}\nu} e^{i\mathbf{q}\cdot\mathbf{r}} \Delta_{\mathbf{q}\nu} v(\mathbf{r};\ \mathbf{R}_0) Q_{\mathbf{q}\nu}(t) l_{\mathbf{q}\nu}^{-1}. \tag{S20}$$

By combining Eq. (S13), (S20) and (S2), we have

$$\begin{aligned} H^{ep}_{m\mathbf{k}',n\mathbf{k}} &= N_p^{-1/2} \sum_{\mathbf{q}\nu} N_p^{-1} \langle u_{m\mathbf{k}'} | e^{-i(\mathbf{k}'-\mathbf{k}-\mathbf{q})\cdot\mathbf{r}} \Delta_{\mathbf{q}\nu} v(\mathbf{r};\ \mathbf{R}_0) | u_{n\mathbf{k}} \rangle\, Q_{\mathbf{q}\nu}(t) l_{\mathbf{q}\nu}^{-1} \\ &= N_p^{-1/2} \sum_{\mathbf{q}\nu} \langle u_{m\mathbf{k}'} | \Delta_{\mathbf{q}\nu} v(\mathbf{r};\ \mathbf{R}_0) | u_{n\mathbf{k}} \rangle_{\mathrm{uc}}\, \delta_{\mathbf{q},\mathbf{k}'-\mathbf{k}} Q_{\mathbf{q}\nu}(t) l_{\mathbf{q}\nu}^{-1} \\ &= N_p^{-1/2} \sum_{\nu} g_{mn\nu}(\mathbf{k},\mathbf{q}) Q_{\mathbf{q}\nu}(t) l_{\mathbf{q}\nu}^{-1} \Big|_{\mathbf{q}=\mathbf{k}'-\mathbf{k}}, \end{aligned} \tag{S21}$$

where the inner-product in the first line is an integral over the entire BvK supercell. Similar to the proof of Eq. (S4), one can show that the integral can be converted to an integral over the unit cell, provided that the momentum is conserved. $g_{mn\nu}(\mathbf{k},\mathbf{q})$ is referred to as the *e-ph* matrix element

$$g_{mn\nu}(\mathbf{k},\mathbf{q}) = \langle u_{m\mathbf{k}+\mathbf{q}} | \Delta_{\mathbf{q}\nu} v(\mathbf{r};\ \mathbf{R}_0) | u_{n\mathbf{k}} \rangle_{\mathrm{uc}}\,. \tag{S22}$$

3 Surface Hopping

The fewest-switches surface hopping (FSSH) method represents time-evolving electron-nuclear system by an ensemble of trajectories, propagating under the influence of deterministic (via TDSE) and stochastic [via surface hopping(SH)] factors. Evolution of the system of interest is defined in a joint space combining classical phase-space for nuclei and discrete quantum states for electrons. The paths are constructed such that the FSSH probabilities for all states at all times, averaged over the trajectory ensemble, are equal to the corresponding probabilities obtained from the TDSE. The latter are given by diagonal

elements of the density matrix:

$$\rho_{m\mathbf{k}',n\mathbf{k}}(t) = c^*_{m\mathbf{k}'}(t)c_{n\mathbf{k}}(t). \tag{S23}$$

The off-diagonal elements determine the probabilities of transitions between electronic states. For simplicity, we take the diagonal elements $\rho_{n\mathbf{k},n\mathbf{k}}$ as $\rho_{n\mathbf{k}}$ following. If the system is in state $n\mathbf{k}$ at time t, then the probability to leave this state at time $t + \Delta t$ is:

$$P_{n\mathbf{k}}(t;\ t+\Delta t) = \frac{\rho_{n\mathbf{k}}(t) - \rho_{n\mathbf{k}}(t+\Delta t)}{\rho_{n\mathbf{k}}(t)} = -\frac{\int_t^{t+\Delta t} \dot{\rho}_{n\mathbf{k}}(t)dt}{\rho_{n\mathbf{k}}(t)}. \tag{S24}$$

From the definition of the density matrix, and from the TDSE, it follows that:

$$\dot{\rho}_{n\mathbf{k}}(t) = \sum_{m\mathbf{k}'} -\frac{2}{\hbar}\,\mathrm{Im}\left(\rho^*_{m\mathbf{k}',n\mathbf{k}} H^{ep}_{m\mathbf{k}',n\mathbf{k}}\right). \tag{S25}$$

Splitting the resulting hopping probability into various channels, $m\mathbf{k}'$, one obtains the probability of transition between the pair of states $n\mathbf{k} \to m\mathbf{k}'$:

$$P_{n\mathbf{k}\to m\mathbf{k}'}(t;\ t+\Delta t) = \frac{2}{\hbar}\frac{\int_t^{t+\Delta t} \mathrm{Im}\left(\rho^*_{m\mathbf{k}',n\mathbf{k}} H^{ep}_{m\mathbf{k}',n\mathbf{k}}\right) dt}{\rho_{n\mathbf{k}}(t)}. \tag{S26}$$

Note that each transition from $n\mathbf{k}$ to $m\mathbf{k}'$ corresponds to one *e-ph* scattering process, where the energy and crystal momentum must be conserved. However, Eq. (S26) can not guarantee the conservation law. To explicitly introduce the conservation law into the probability equation, recall that Fermi's golden rule gives the transition rate between two states

$$\begin{aligned}\frac{\mathrm{d}}{\mathrm{d}t}\mathcal{P}_{n\mathbf{k}\to m\mathbf{k}'}(t) =& \frac{2\pi}{\hbar}|H^{ep}_{m\mathbf{k}',n\mathbf{k}}|^2 \times \\ & \left[\delta(\epsilon_{m\mathbf{k}'} - \epsilon_{n\mathbf{k}} - \hbar\omega_{\mathbf{q}\nu}) + \delta(\epsilon_{m\mathbf{k}'} - \epsilon_{n\mathbf{k}} + \hbar\omega_{\mathbf{q}\nu})\right].\end{aligned} \tag{S27}$$

As a result, the modified hopping probability equation changes to

$$\tilde{P}_{n\mathbf{k}\to m\mathbf{k}'}(t;\ t+\Delta t) = \frac{2}{\hbar}\frac{\mathrm{Im}\left(\rho^*_{m\mathbf{k}',n\mathbf{k}}(t)\tilde{H}^{ep}_{m\mathbf{k}',n\mathbf{k}}\right)\Delta t,}{\rho_{n\mathbf{k}}(t)}, \tag{S28}$$

where $\tilde{H}^{ep}_{m\mathbf{k}',n\mathbf{k}}$ is given by

$$\begin{aligned}\tilde{H}^{ep}_{m\mathbf{k}',n\mathbf{k}} =& \frac{2\pi}{N_p}\sum_{\nu}|g_{mn\nu}(\mathbf{k},\mathbf{q})|^2(n_{\mathbf{q}\nu} + \frac{1}{2}) \times \\ & \left[\delta(\epsilon_{m\mathbf{k}'} - \epsilon_{n\mathbf{k}} - \hbar\omega_{\mathbf{q}\nu}) + \delta(\epsilon_{m\mathbf{k}'} - \epsilon_{n\mathbf{k}} + \hbar\omega_{\mathbf{q}\nu})\right].\end{aligned} \tag{S29}$$

where the two δ function correspond to absorbing and emitting of phonon, respectively. In practical implementation, however, Gaussian function with certain broadening σ is used to approximate the Dirac δ-function

$$\delta(E) \approx \frac{1}{\sigma\sqrt{2\pi}} e^{-\frac{E^2}{2\sigma^2}}. \tag{S30}$$

If the computed probability is negative, it is reset to zero. Thus, in general, the FSSH assigns a probability for transition from the current electronic state $n\mathbf{k}$ to the new state $m\mathbf{k}'$, as:

$$g_{n\mathbf{k}\to m\mathbf{k}'}(t;\ t+\Delta t) = \max\left[0, \tilde{P}_{n\mathbf{k}\to m\mathbf{k}'}(t;\ t+\Delta t)\right], \tag{S31}$$

$$g_{n\mathbf{k}\to n\mathbf{k}}(t;\ t+\Delta t) = 1 - \sum_{m\mathbf{k}'\neq n\mathbf{k}} g_{n\mathbf{k}\to m\mathbf{k}'}(t;\ t+\Delta t). \tag{S32}$$

In order to reflect the detailed balance condition, the hop rejection and velocity rescaling of the standard FSSH are replaced in the FSSH-CPA by scaling the transition probabilities $g_{n\mathbf{k}\to n\mathbf{k}}$ with the Boltzmann factor:

$$g_{n\mathbf{k}\to m\mathbf{k}'} \quad \Rightarrow \quad g_{n\mathbf{k}\to m\mathbf{k}'} b_{n\mathbf{k}\to m\mathbf{k}'}, \tag{S33}$$

$$b_{n\mathbf{k}\to m\mathbf{k}'} = \begin{cases} \exp\left(-\frac{\epsilon_{m\mathbf{k}'}-\epsilon_{n\mathbf{k}}}{k_B T}\right) & \epsilon_{m\mathbf{k}'} > \epsilon_{n\mathbf{k}} \\ 1 & \epsilon_{m\mathbf{k}'} \leq \epsilon_{n\mathbf{k}} \end{cases}. \tag{S34}$$

4 Test of k-grid Size and Energy Broadening

In graphene, the Dirac conical band structure results in a very small density of electronic states near the Fermi level (E_f), so a sufficiently dense $\mathbf{k}$-grid is required to accurately model the hot electron relaxation process. We have tested the simulation of hot electron relaxation with different $\mathbf{k}$-grid sizes, as shown in Fig. S1. It can be seen that with the increase of $\mathbf{k}$-point density, the electron relaxation process gradually converges. When the density of $\mathbf{k}$-points reaches $90 \times 90 \times 1$, the change of the hot electron relaxation process becomes negligible. However, it should be noted that as the electron energy gets closer to the Dirac point, the density of its electronic states decreases, so a denser $\mathbf{k}$-point is required. Hence, we use the $\mathbf{k}$-point grid of $150 \times 150 \times 1$ in simulations for $E_{\text{ini}} = 0.4 - 1.5\,\text{eV}$, and $\mathbf{k}$-point grid of $450 \times 450 \times 1$ in simulations for $E_{\text{ini}} < 0.3\,\text{eV}$.

In the *e-ph* coupling with energy conservation correct, to choose a reasonable energy broadening, we have tried different σ values to simulate the hot electron dynamics with initial energy of 1.0 eV ($E_{\text{ini}} = 1.0\,\text{eV}$). As shown in Fig. S2, the electron dynamics gets more and more elaborate as the energy broadening decreases 500 to 5 meV, while the relaxation time barely changes.

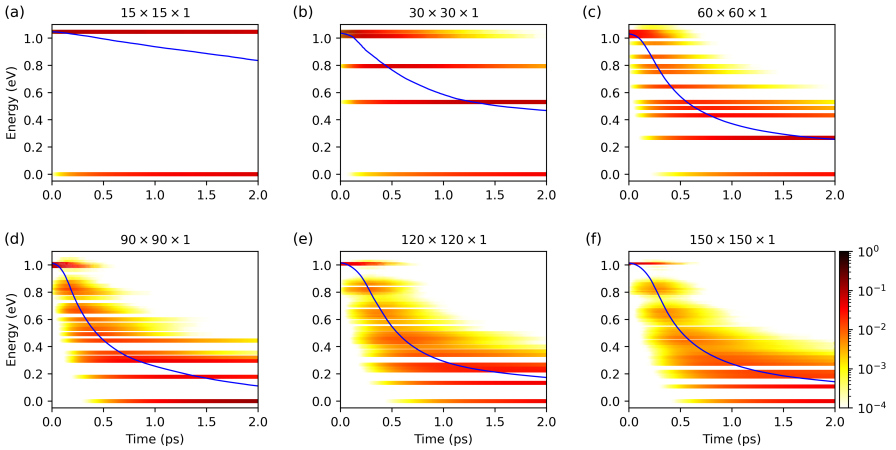

Fig. S1 Hot electron dynamics ($E_{ini} = 1.0\,\text{eV}$) with **k**-points grid of (a) $15 \times 15 \times 1$, (b) $30 \times 30 \times 1$, (c) $60 \times 60 \times 1$, (d) $90 \times 90 \times 1$, (e) $120 \times 120 \times 1$, and (f) $150 \times 150 \times 1$. The color dots indicate the electron population in different states, and the blue line represents the averaged electron energy.

We can also find that the relaxation is blocked at low energy region for energy broadening is smaller than 10 meV. That is due to the finite **k**-grid, which causes energy gap between different electronic states. To simulate the carrier relaxation in energy bands with continuous **k**-grid, usually a smaller σ will provide more accurate results if the **k**-grid sampling is dense enough. In this article we use $\sigma = 25$ meV. To simulate the carrier dynamics across a band gap, the σ value can be estimated by the thermal oscillation of the electronic state at a certain temperature.

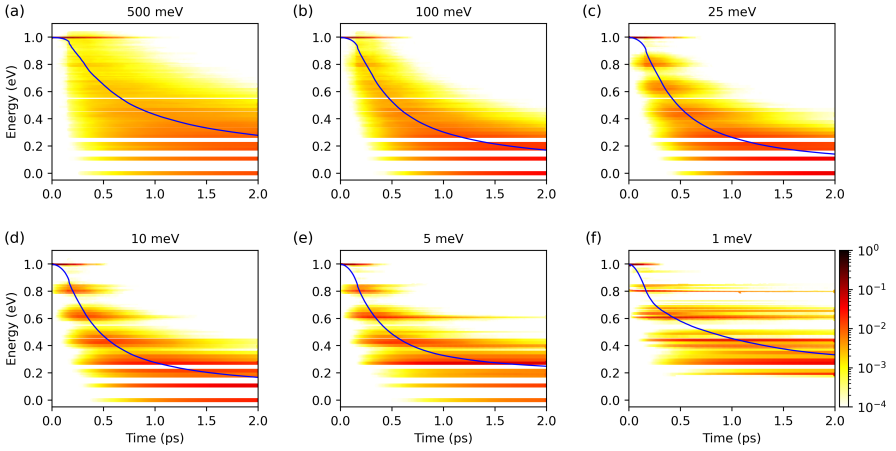

Fig. S2 Hot electron dynamics ($E_{\text{ini}} = 1.0\,\text{eV}$) with energy broadening of (a) 500 meV, (b) 100 meV, (c) 25 meV, (d) 10 meV, (e) 5 meV, and (f) 1 meV. The color dots indicate the electron population in different states, and the blue line represents the averaged electron energy.

5 Comparison with NAMD simulation in real space (NAMD_r)

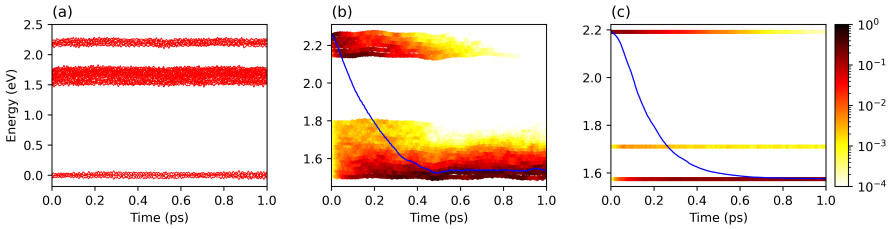

Fig. S3 (a) Energy evolution of KS states in the NAMD_**r** approach. The hot electron relaxation simulation from 2.2 eV to 1.6 eV using (b) NAMD_**r** method with $9 \times 9 \times 1$ supercell and (c) NAMD_**k** method with $9 \times 9 \times 1$ k-grid. The color dots indicate the electron population in different states, and the blue line represents the averaged electron energy.

In order to verify the validity of the NAMD_**k** method, we compare the calculation results of the NAMD_**k** with the NAMD_**r** approach. In the NAMD_**r** approach, a supercell is required to sample the phonon excitation with different **q** points. Here we only simulate a $9 \times 9 \times 1$ supercell due to the limitation of computational cost. Then we compare the results with what NAMD_**k** obtains using $9 \times 9 \times 1$ **k**-grid. As the energy gaps are large for the $9 \times 9 \times 1$ supercell or **k**-grid close to the Fermi level, we choose to simulate the process of hot electron evolving from 2.2 eV to 1.6 eV, where the energy gaps are smaller relatively. As shown in Fig. S3, the states in NAMD_**k** simulation degenerate to 3 energy levels because we use the eigenstates of equilibrium structure Hamiltonian, and in fact the number of states equals to the NAMD_**r** simulation. Based on the NAMD_**r** simulation on graphene with $9 \times 9 \times 1$ supercell, we estimate the σ value to be 120 meV from the thermal oscillation. The results obtained by NAMD_**r** and NAMD_**k** agree with each other in substance. It clearly proves the validity of the NAMD_**k** approach.